Long-Endurance Sensing and Mapping using a Hand-Launchable Solar-Powered UAV

Conference Paper

Author(s):
Oettershagen, Philipp; Stastny, Thomas; Mantel, Thomas; Melzer, Amir; Rudin, Konrad; Gohl, Pascal; Agamennoni, Gabriel; Alexis, Kostas; Siegwart, Roland

Long-Endurance Sensing and Mapping using a Hand-Launchable Solar-Powered UAV

Philipp Oettershagen, Thomas Stastny, Thomas Mantel, Amir Melzer, Konrad Rudin, Pascal Gohl, Gabriel Agamennoni, Kostas Alexis, and Roland Siegwart

Abstract This paper investigates and demonstrates the potential for very long endurance autonomous aerial sensing and mapping applications with AtlantikSolar, a small–sized, hand–launchable, solar–powered fixed–wing unmanned aerial vehicle. The platform design as well as the on–board state estimation, control and path–planning algorithms are overviewed. A versatile sensor payload integrating a multi–camera sensing system, extended on–board processing and high–bandwidth communication with the ground is developed. Extensive field experiments are provided including publicly demonstrated field–trials for search–and–rescue applications and long–term mapping applications. An endurance analysis shows that AtlantikSolar can provide full-daylight operation and a minimum flight endurance of 8 hours throughout the whole year with its full multi-camera mapping payload. An open dataset with both raw and processed data is released and accompanies this paper contribution.

1 Introduction

The field of aerial robotics has seen rapid growth in the last decade. Prerequisite technologies have developed to the point that we are not far from the day when utilization of aerial robots is prevalent in our society. With an application range that includes infrastructure inspection [13], surveillance for security tasks [6], disaster relief [25, 8], crop monitoring [7], mapping [1], and more, Unmanned Aerial Vehicles (UAVs) already provide added value to several critical and financially significant applications, and are widely acknowledged for their potential to achieve a large impact in terms of development and growth. Examples of compelling existing use–cases include the mapping of the Colorado flood area in 2003 [4], the 3D reconstruction of the "Christ the Redeemer" statue in Brazil and the Matterhorn mountain

Autonomous Systems Lab, ETH Zurich, Switzerland, e-mail: philipp.oettershagen@mavt.ethz.ch

reconstruction [20], and the live offshore flare inspection that took place in the North Sea [3].

While these are impressive achievements, there are still major factors that limit the applicability of UAVs. One such factor is their relatively low endurance. Indeed, long–endurance flight capabilities are crucial for applications such as large-scale Search–and–Rescue support, industrial pipeline monitoring, atmospheric research, offshore inspection, precision agriculture and wildlife monitoring. This new class of problems exposes a practical limitation in the majority of currently available aerial robot configurations.

Solar–powered flight is a key enabling technology for long-endurance operations. By harnessing the suns energy and storing solar power during the day, flight times can be significantly prolonged. In cases of extreme designs, sustained flight can even be achieved through night time and/or cloudy conditions. An existing example of extreme endurance is the QinetiQ Zephyr UAV (22 m wingspan), which broke records, sustaining flight for two weeks [24]. However, scaling down from the high-altitude "pseudo satellite" class to more manageable, rapidly deployable and low-altitude designs is not trivial.
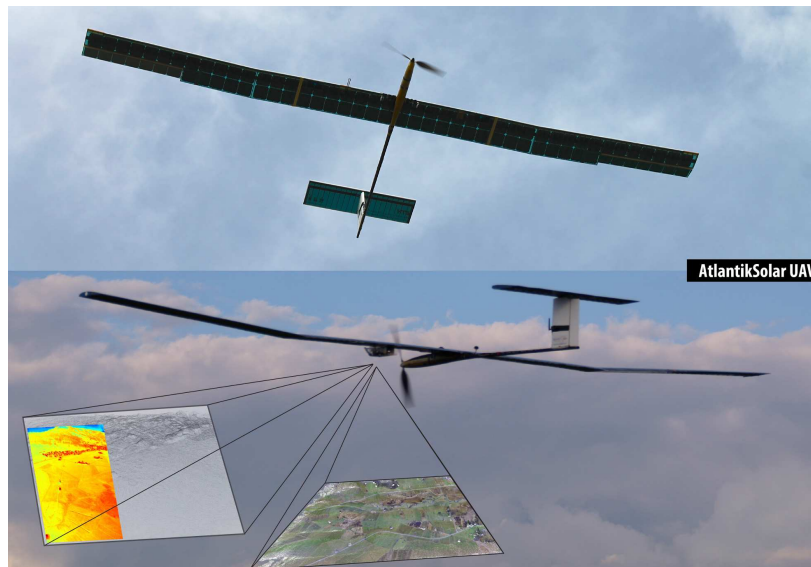

Fig. 1 The AtlantikSolar UAV is capable of very long–endurance operation in missions including mapping, surveillance, victim detection and infrastructure inspection.

Motivated by the increasing industrial, scientific and societal demand for persistent automatic aerial sensing and surveillance, long–endurance, solar–powered fixed–wing aircrafts have been a research priority in the Autonomous Systems Lab (ASL) at ETH Zurich. With the most recent development being the AtlantikSolar UAV, our aim is to extend the current technological state of the art with a robust

and versatile platform capable of significantly longer term sensing and mapping on the order of days or even weeks. Fig. 1 depicts the AtlantikSolar UAV and its sensing capabilities. The detailed design of this UAV platform has been described in [18]. This paper extends our previous design-oriented work by investigating and characterizing possible application scenarios for our platform. More specifically, we present a set of field trials that are enabled by a diverse sensor payload recently integrated into the UAV. This on–board sensor payload includes RGB and grayscale camera systems and a thermal vision sensor in combination with a complete suite of sensors that enable the vehicle to navigate autonomously.

The remainder of this paper is organized as follows: We present a description of the AtlantikSolar vehicle in Section 2, its sensing and mapping capabilities in Section 3, field experiment results in Section 4, and derived conclusions in Section 5. We also provide a detailed discussion of our experiences from both search–and–rescue as well as mapping missions, and release a dataset containing raw as well as post–processed data.

2 AtlantikSolar Unmanned Aerial Vehicle
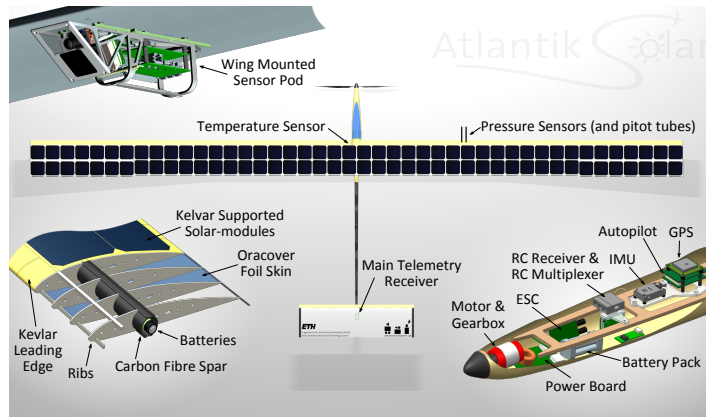
2.1 Platform Overview

Fig. 2 AtlantikSolar system overview.

The AtlantikSolar UAV (Fig. 2, Table 1) is a small-sized, hand-launchable, low-altitude long-endurance (LALE), solar-powered UAV optimized for large-scale aerial mapping and inspection applications. A detailed overview of the conceptual design of AtlantikSolar is given in [18]. The design methodology is based on the work in [16, 10] with extensions on optimizing solar-powered UAVs for a range of deteriorated meteorological conditions (e.g. cloud obstruction of sun radiation) as

given in [18] . The platform owes much of its configuration to the optimization of power consumption. Lightweight composite materials are used in the fabrication of a torsionally resistant cylindrical carbon fibre spar, tapered carbon fibre tail boom, and fibreglass fuselage body. The AtlantikSolar prototype UAV used for the flight tests in this paper features 88 SunPower $E60$ cells with an efficiency of $\eta_{sm} = 0.23$. Energy is stored in 2.9 kg of cylindrical high energy density Li-Ion batteries (Panasonic NCR18650b, 243 Wh kg^{-1}, 700 Wh total) that are integrated into the wing spar for optimal weight distribution. The two ailerons, the elevator and the rudder are driven by brushless Volz DA-15N actuators with contactless position feedback. The propulsion system consists of a foldable custom-built carbon-fibre propeller, a 5:1 reduction gearbox and a 450 W brushless DC motor.

Table 1 Summary of AtlantikSolar design and performance characteristics.

Specification	Value/Unit
Wing span	5.65 m
Mass	7.5 kg
Nominal cruise speed	9.7 m s^{-1}
Max. flight speed	20 m s^{-1}
Min. endurance (no payload)[a]	13 h
Design endurance (no payload)	10 d

[a] on battery-power only

A Pixhawk PX4 Autopilot, an open source/open hardware project started at ETH Zurich [21], is the centerpiece of the avionics system. It employs a Cortex M4F microprocessor running at 168Mhz with 192kB RAM to perform autonomous flight control and state estimation. Major hardware modifications include the integration of the ADIS16448 IMU and the Sensirion SDP600 differential pressure as well as re–writing of the estimation and control algorithms.

2.2 Operational Concept

AtlantikSolar is hand-launched to enable rapid deployment and operation in remote or uneven terrain. It is operated by a two-person team consisting of the safety-pilot and an operator for high-level mission management through the ground control station (GCS) interface (QGroundControl [23]). The GCS allows automatic loitering and autonomous waypoint following of user-defined or pre-computed paths. For visual-line-of-sight operation, the primary (434 MHz) telemetry link is sufficient, but an Iridium satellite link is also integrated to act as a backup link in the event of primary radio loss or beyond-visual-line-of-sight operation (Fig. 3). The UAV is equipped with a wing-mounted sensor pod, but provides additional payload capacity and versatility within its total payload budget of $m_{pld,max} \approx 800g$. AtlantikSolar also integrates four high-power LEDs for night operations.

Fig. 3 Communications and ground control.

2.3 Enabling Technologies for Autonomous Navigation

2.3.1 Robust Long-Term State Estimation

To provide reliable and drift-free long-term autonomous operation, a light-weight EKF-based state estimator, as presented in [11], is implemented on the autopilot. It fuses data from a 10-DoF Inertial Measurement Unit (IMU) with GPS-Position, GPS-velocity and airspeed measurements in order to successively estimate position, velocity, orientation (attitude and heading), QFF as well as accelerometer and gyro biases. Robustness against temporal GPS losses is enhanced through the inclusion of airspeed measurements from a differential barometer. To increase flight safety, the algorithm estimates the local three-dimensional wind vector and employs an internal aircraft aerodynamics model to estimate the current sideslip angle and Angle of Attack (AoA), which can in turn be used by the flight controller to apply implicit flight regime limits, as in the case of the authors' previous work [17].

2.3.2 Flight Control

AtlantikSolar's flight control system features automatic tracking of waypoints along pre-defined paths, allows extended loitering around areas of interest and implements safety-mechanisms such as automatic Return-To-Launch (RTL) in case of prolonged remote control or telemetry signal losses. The baseline control is a set of cascaded PID-controllers for inner-loop attitude control [2]. Output limiters are applied to respect the aircraft flight envelope, dynamic pressure scaling of the control outputs is used to adapt to the changing moment generation as a function of airspeed and a

coordinated-turn controller allows precise turning. Altitude control is based on a Total Energy Control System that also allows potential energy gains in thermal updraft while it implements safety mechanisms such as automatic spoiler deployment during violation of maximum altitude limits. Waypoint-following is performed using an extended version of the $\mathcal{L}_1$-nonlinear guidance logic [19]. The detailed implementation and verification of our autopilot is described in [18].

2.3.3 Inspection Path–Planner

An inspection path–planning algorithm is integrated into the system in order to enable automated inspection and mapping of large scale 3D environments. The algorithm is inherently tailored for structural inspection and computes full coverage and collision–free paths subject to a model of the nonholonomic constraints of the vehicle. The overall approach is illustrated in Fig. 4, while a detailed description is available in the authors' previous work [1]. It essentially corresponds to an explicit algorithm that computes an inspection path based on a mesh–model representation of the desired world. It iteratively tries to compute viewpoint configurations that provide full coverage while at the same time employing the Lin-Kernighan heuristic [12] in the search for the best route that visits all of them subject to the motion constraints of the vehicle. Via a viewpoint resampling technique that employs randomized sampling, the designed algorithm allows for an iterative improvement of the path cost while always retaining complete coverage. Fast collision–free navigation is achieved via a combination of a Boundary Value Solver for the considered vehicle model with the RRT* [9] motion planner.
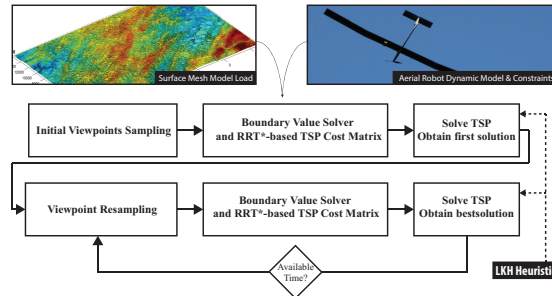

Fig. 4 Summary of the employed 3D inspection path–planning algorithm.

3 Sensor Pod

The sensor pod (see Fig. 5) features a grayscale (Aptina MT9V034) camera with a high dynamic range and a long-wavelength infrared (LWIR) camera (FLIR Tau 2) for thermal imaging, both mounted with an oblique field of view (FOV), as well as a nadir facing RGB camera (uEye XS 2). An IMU (Analaog Devices ADIS16448) is also included, measuring linear accelerations, angular velocities, and the magnetic field in all three axes. All sensors are integrated with a Skybotix VI-sensor [27], allowing tight hardware synchronization and timestamping of the acquired data [15]. Furthermore, a state of the art embedded computer (Kontron COMe-mBT10), with an Intel Atom CPU (4 cores, 1.91 GHz) and a thermal design power (TDP) of 10 W, is interfaced with the VI-sensor and the PX4 autopilot board of the UAV. The on–board Atom computer further communicates with the PX4 in order to receive all global pose estimates and raw sensor data and transmit waypoints. The acquired data is processed on–board and communication with the ground control station is achieved over Wi–Fi. As shown in Fig. 5, all components are mounted on a lightweight aluminum construction ensuring a rigid connection between the cameras and the IMU, thus guaranteeing high quality extrinsic calibration of the sensors, a key element for accurate visual-inertial localization.
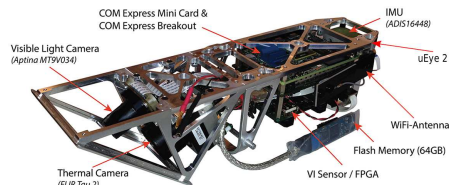

Fig. 5 The sensor pod as it is currently used on the AtlantikSolar without fairing for better visibility of the components.

The on-board computer runs a standard Ubuntu Linux operating system, allowing quick adaptation to different kinds of missions. Furthermore, it enables rapid testing of new algorithms, e.g. for localization and mapping. It has been utilized to evaluate monocular localization [10] while the original stereo version of the VI–sensor is actively used for localization of rotary–wing UAVs in possibly GPS–denied environments [14]. Within the framework of the research projects ICARUS and SHERPA [8, 26], the described sensor pod is used for area mapping, victim detection, and situational awareness tasks. The data of the visible light cameras is combined with the pose estimates and fed to post–processing software [20] to derive accurate 3D reconstructions of the environment. Active research is ongoing for aerial victim detection at altitudes on the order of 100 m.

4 Flight Experiments

AtlantikSolar is a key component of several research projects and has actively partic-ipated in multiple large–scale demonstration events. Within this paper, indicative re-sults from the ICARUS project [8] public field–trials event at Marche–en–Famenne, Belgium and a long–endurance mapping mission in Rothenthurm, Switzerland are presented along with flight endurance related tests and evaluations. A dataset is also released and documented to accompany this paper. It contains the vehicle state es-timates, IMU and GPS raw data, the camera frames from all the on–board modules as well as post–processed reconstructions of the environment for the field–trials de-scribed in Section 4.2. This rich dataset is publicly available at [5].

4.1 Search–and–Rescue Application Demonstration

During the ICARUS project field–trials in Marche–en–Famenne [8], the AtlantikSo-lar UAV was commanded to autonomously execute inspection paths that ensured the complete coverage of a predefined area in order to assist the area monitoring, map-ping, victim detection and situational awareness necessities of Search–and–Rescue rapid response teams. Employing the path–planner overviewed in Section 2.3.3 and based on the long–endurance capabilities of the UAV, the area was scanned repeat-edly over multiple hours. An example inspection path is depicted in Fig. 6 and cor-responds to an optimized solution for the case of the oblique–view mounted ther-mal camera, FOV $(56°, 60°)$ for the horizontal and vertical axes, respectively. The mounting orientations of the grayscale and the thermal camera are identical, but the FOV of the grayscale camera is larger in all directions $(70°, 100°)$, thus the planned path provides full coverage for both vision sensors.

   During the execution of these inspection paths, the two camera–system and the pose estimates of the aircraft were uniformly timestamped and recorded in a ROS bag. Subsequently, post–processing of the grayscale images was conducted in order to derive a dense point–cloud of the area using the Pix4D software [20]. An image of the derived result is shown in Fig. 7, while additional results of autonomously executed inspection paths may be found in our previous work [1].

4.2 Area Coverage Application Demonstration

In this specific field experiment, the AtlantikSolar UAV's capabilities for long–term area coverage, inspection and mapping were evaluated. Within 6 hours of flight, the system performed multiple lawn–mowing and other paths like those presented in Fig. 8. With a camera frame recording rate set at $F_c = 1$Hz, synchronization with the vehicle pose estimates and properly designed waypoint distances to ensure coverage and sufficient overlap for all cameras, a solid reconstruction result was

Fig. 6 Inspection path full area coverage using the oblique–view mounted thermal vision and grayscale cameras of the AtlantikSolar sensor pod. The colored mosaic was derived using an additional very large field of view nadir–facing camera (HDR-AS100VW).

Fig. 7 Reconstructed dense point cloud based on the combination of the oblique–view grayscale camera images with the vehicle position estimates. The reconstruction was achieved using the Pix4D mapping software.

achieved. Within this flight, all three cameras were employed and Fig. 9 depicts the reconstructed point cloud using a combination of the geo–tagged nadir–facing RGB camera of the sensor pod with the, likewise, geo–tagged oblique–view grayscale images, while Fig. 10 shows false–colored thermal images that our team is currently aiming to employ for victim detection, extending previous work [22] at ASL. An open dataset containing 1 hour of raw data and post–processed results is released to accompany this paper and may be found at [5].
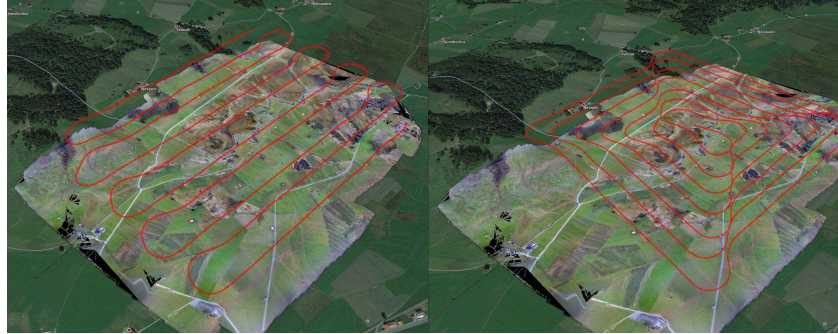
Fig. 8 The lawn–mowing path executed by the AtlantikSolar UAV overlayed on the reconstructed mosaic of the environment, incorporated in Google maps.
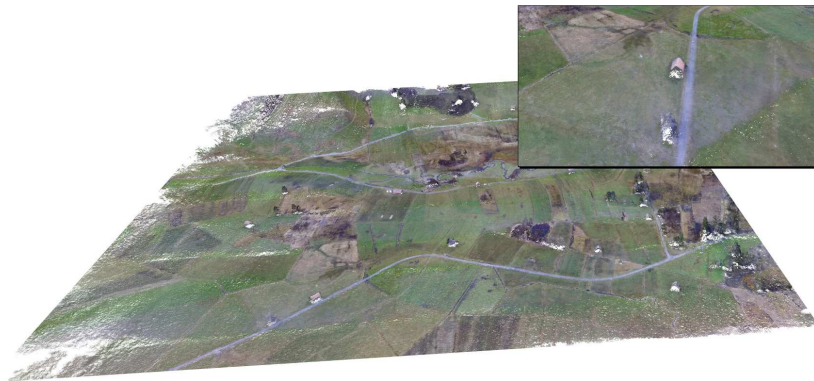

Fig. 9 The reconstructed point–cloud of the Rothenthurm area based on the combination of the RGB and grayscale camera data as well as the UAV pose estimates collected during the lawn–mowing path and subsequently processed using the Pix4D software.
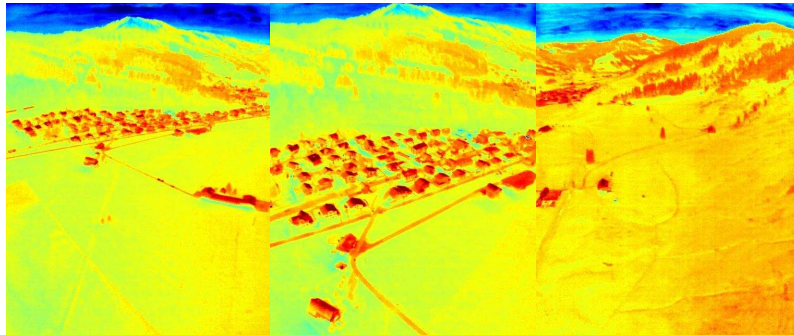

Fig. 10 False–colored thermal camera images recorded using the on–board sensor pod of the AtlantikSolar UAV.

4.3 Full-Payload Flight Endurance and Range

After having shown a flight endurance of more than 12 hours without payload in Summer 2014 [18], the area coverage demonstration in Rothenthurm on November 21st was used to determine AtlantikSolar's maximum flight endurance with the full sensor pod payload of $m_{payload} = 610g$ during winter conditions. Fig. 11 shows the corresponding power income, output, and battery state. The average power consumption during the flight is $P_{aircraft} = 69.7W$ plus $P_{payload} = 15W$ for the sensor pod. After take-off at 10:25am local time at 94% battery state-of-charge (SoC), the heavily attitude-dependent solar power income increases but reaches only a maximum of 80W at noon due to the limited insolation in winter. Nevertheless, as indicated by the SoC, the system power is mostly drawn from the solar panels for more than 3 hours of the flight. Power income decreases towards the afternoon: The solar panel maximum power point trackers (MPPTs) are still operating, but the panel voltage has decreased significantly and the MPPTs deliver currents below the measurement threshold. However, the remaining SoC during landing shortly before sunset (4:28pm local time) is still 52%. Extrapolating using the total power consumption of $P_{tot} = P_{aircraft} + P_{payload} = 69.7W + 15W = 84.7W$ yields an additional 4.32 hours of remaining flight endurance assuming zero-radiation conditions and thus a total flight endurance of ca. 10h with full payload for the installed 700Wh battery during these winter conditions.
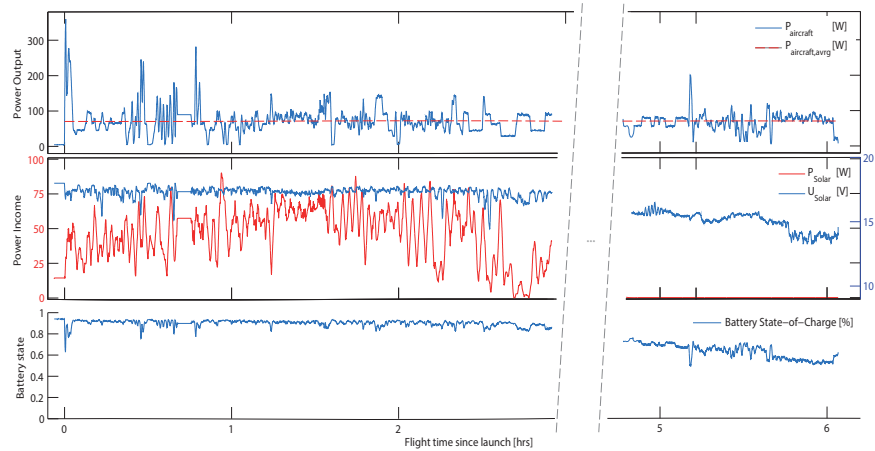

Fig. 11 Power income, output and battery state-of-charge for the Rothenthurm mapping flight. AtlantikSolar covered 243km ground-distance, was airborne for 6 hours 3 minutes and landed shortly before sunset (4:28pm local time) with 52% battery capacity remaining.

The recorded power consumption of $P_{tot} = 84.7W$ was taken as the input for the flight endurance simulation in Fig. 12. Assuming launch of the airplane exactly at sunrise, full-daylight flight endurance is provided throughout the full year including

winter under most atmospheric conditions. More specifically, full-daylight flight capability is only lost when $CLR = P_{Solar}/P_{Solar,ClearSky}$ is smaller than ca. 0.3 in summer and ca. 0.15 in winter, which corresponds to severe cloud coverage or fog that may hinder flight operations independently of energy considerations. The maximum endurance of AtlantikSolar with the full payload is 22.4 hours on June 21st, which means that perpetual flight is not possible. Note that in all atmospheric conditions, a minimum endurance of 8 hours can be guaranteed through battery-powered flight alone. At the chosen airspeed of $v_{air} = 11.02m/s$, AtlantikSolar can thus cover a ground distance of 317km (min. endurance) to 888km (max. endurance). Note that this airspeed provides the maximum range (optimal glide ratio), but is not the power-optimal airspeed (lowest rate of sink). Flying strictly at the power-optimal airspeed found in [18] would e.g.increase the endurance to 23.9 hours on June 21st, with battery energy depleting shortly before sunrise. This means that perpetual flight with the full sensor payload can theoretically be achieved through minor aircraft optimizations, e.g. through a slight increase of the available battery capacity. However, note increasing endurance through power-optimal airspeed selection in the non-perpetual flight endurance case comes at a cost of range, and should be considered per application.
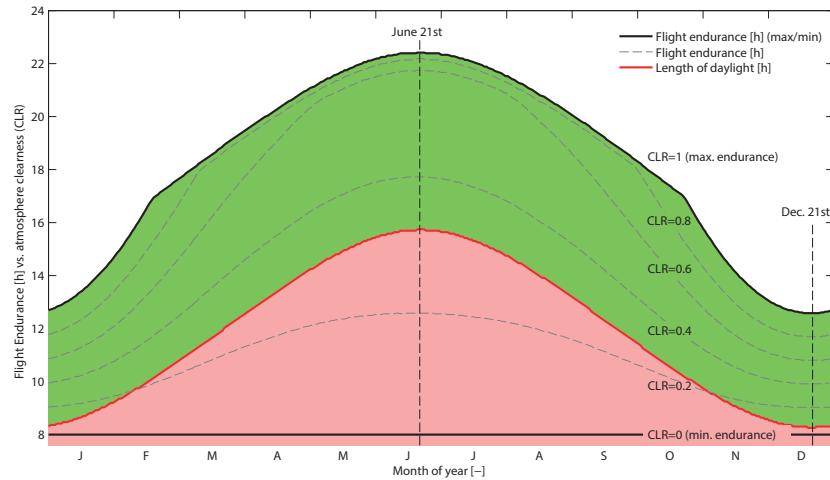

Fig. 12 AtlantikSolar's flight endurance with 610g/15W payload versus atmospheric clearness (CLR) for $\phi = 47^o N$ (Rothenthurm, CH) when assuming launch at sunrise with SoC=100%. Full daylight flight is possible throughout the whole year (green area), and only severe cloud coverage can reduce endurance below the daylight duration (red area). In all cases 8 hours of minimum endurance are achieved.

5 Conclusions

In this work, we have demonstrated a significant leap in long–endurance, low–altitude aerial sensing and mapping. Utilizing optimized solar aircraft design methodologies, low power consumption electronics, a robust autonomous navigation framework, and a versatile, modular, and self-contained sensor payload, the AtlantikSolar system, as a whole, provides a baseline to address quickly approaching societal needs related to long-term aerial robotic operations. Extensive field–trial experience indicates that solar power is a promising solution towards providing long endurance to small–sized, low–altitude UAVs, and integrated sensor suites, when used in tandem with autonomous navigation and planning methods, can provide wealth of valuable information to end users in an efficient manner. Still, there is great room for improvement, especially in the directions of autonomous navigation close to terrain, where a combination of advanced perception and planning algorithms have to be employed. Also in terms of superior robustness, as required for multi–hour or even multi–day flight.

References

[1] Bircher A, Alexis K, Burri M, Oettershagen P, Omari S, Mantel T, Siegwart R (2015) Structural inspection path planning via iterative viewpoint resampling with application to aerial robotics. In: Robotics and Automation (ICRA), 2014 IEEE International Conference on, (accepted)

[2] Brian L Stevens and Frank L Lewis (1992) Aircraft Control and Simulation. Wiley Interscience

[3] Cyberhawk - Remote aerial inspection and land surveying specialists (2015) http://www.thecyberhawk.com/

[4] Falcon UAV (2015) http://www.falconunmanned.com/

[5] FSR 2015 - Solar-powered UAV Sensing and Mapping Dataset (2015) http://projects.asl.ethz.ch/datasets/doku.php?id=fsr2015

[6] Girard A, Howell A, Hedrick J (2004) Border patrol and surveillance missions using multiple unmanned air vehicles. In: Decision and Control, 2004. CDC. 43rd IEEE Conference on

[7] Hunt ER, Hively WD, Fujikawa SJ, Linden DS, Daughtry CST, McCarty GW (2010) Acquisition of nir-green-blue digital photographs from unmanned aircraft for crop monitoring. Remote Sensing 2(1):290–305

[8] ICARUS: Unmanned Search and Rescue (2015) http://www.fp7-icarus.eu/

[9] Karaman S, Frazzoli E (2010) Incremental sampling-based algorithms for optimal motion planning. CoRR abs/1005.0416

[10] Leutenegger S (2014) Unmanned solar airplanes: Design and algorithms for efficient and robust autonomous operation. PhD thesis, ETH Zurich

[11] Leutenegger S, Melzer A, Alexis K, Siegwart R (2014) Robust state estimation for small unmanned airplanes. In: IEEE Multi-conference on Systems and Control

[12] Lin S, Kernighan BW (1973) An effective heuristic algorithm for the traveling-salesman problem. Operations research 21(2):498–516

[13] Metni N, Hamel T (2007) A UAV for bridge inspection: Visual servoing control law with orientation limits. Automation in Construction 17(1):3–10

[14] Nikolic J, Burri M, Rehder J, Leutenegger S, Huerzeler C, Siegwart R (2013) A UAV System for Inspection of Industrial Facilities. In: IEEE Aerospace Conference

[15] Nikolic J, Rehder J, Burri M, Gohl P, Leutenegger S, Furgale PT, Siegwart RY (2014) A Synchronized Visual-Inertial Sensor System with FPGA Pre-Processing for Accurate Real-Time SLAM. In: IEEE International Conference on Robotics and Automation (ICRA)

[16] Noth A (2008) Design of solar powered airplanes for continuous flight. PhD thesis, ETH Zurich

[17] Oettershagen P, Melzer A, Leutenegger S, Alexis K, Siegwart R (2014) Explicit Model Predictive Control and $\mathscr{L}_1$-Navigation Strategies for Fixed-Wing UAV Path Tracking. In: 22nd Mediterranean Conference on Control & Automation (MED)

[18] Oettershagen P, Melzer A, Mantel T, Rudin K, Lotz R, Siebenmann D, Leutenegger S, Alexis K, Siegwart R (2015) A Solar-Powered Hand-Launchable UAV for Low-Altitude Multi-Day Continuous Flight. In: IEEE International Conference on Robotics and Automation (ICRA)

[19] Park S, Deyst J, How JP (2004) A new nonlinear guidance logic for trajectory tracking. In: AIAA Guidance, Navigation, and Control Conference and Exhibit, pp 16–19

[20] Pix4D (2015) http://pix4d.com/

[21] Pixhawk Autopilot (2015) http://pixhawk.org/

[22] Portmann J, Lynen S, Chli M, Siegwart R (2014) People detection and tracking from aerial thermal views. In: Robotics and Automation (ICRA), IEEE International Conference on, pp 1794–1800

[23] QGroundControl (2015) http://www.qgroundcontrol.org/

[24] QinetiQ (2010) QinetiQ files for three world records for its Zephyr Solar powered UAV. QinetiQ Press Release, retrieved from http://www.qinetiq.com/media/news/releases/Pages/three-world-records.aspx

[25] Rudol P, Doherty P (2008) Human body detection and geolocalization for uav search and rescue missions using color and thermal imagery. In: Aerospace Conference, 2008 IEEE, pp 1–8

[26] SHERPA Project (2015) http://www.sherpa-project.eu/

[27] Skybotix AG (2015) http://www.skybotix.com/